

MR Image Content-Adaptive Finite Element Mesh Generation

W. H. Lee¹, T-S. Kim¹, M. H. Cho¹, S. Y. Lee¹

¹Biomedical Engineering, Functional and Metabolic Imaging Center, Kyung Hee University, Yongin, Kyungki, Korea, Republic of

Introduction

The use of MR images is increasing significantly in various fields including biomechanics, bioelectromagnetics, and biomolecular imaging. Finite element analysis (FEA) provides a powerful analytical means for such use with several advantages over other conventional methods since it allows realistically volumetric analysis and incorporation of material properties. In FEA, mesh generation is the first critical requirement and there exist many methods. However most conventional methods are not effective in handling complex geometry of biological organs, and moreover do not utilize the content of images when generating meshes. In this work, we have developed an effective mesh generation technique producing meshes that are adaptive to the content of MR images. As demonstrated, our mesh generator produces MRI content-adaptive meshes (cMESH) in a fast, automatic, and efficient way which could be utilized in the various fields where MR images provide critical information.

Methods

Our cMESH generation involves the following steps: content-preserving anisotropic diffusion for pre-segmentation of sub-volumes and improvement in the quality of feature maps, generation of feature maps, sampling of content-adaptive nodes, and Delaunay tessellation.

First, morphological processing was applied to remove the background of MR. Second, to remove undesirable objects in the given MR images including noise and artifacts and to pre-segment anatomical regions, the 3-D Gradient Vector Flow (GVF) anisotropic diffusion algorithm was applied [1]. Third, to derive content-adaptive mesh nodes from the filtered MR images, a feature map of the image was derived: in our case, a feature map f (Eq. 1) was derived from the structure tensor S (Eq. 2) derived from MRI, where μ 's are the positive eigenvalues of structure tensor. The feature map reflects the edges and corners of image structures with (+) and the local coherence or anisotropy with (-). The sensitivity of feature map is controlled by the parameter κ (Eq. 3).

$$f_S(i, j) = \sqrt{(\mu_1^S(i, j) \pm \mu_2^S(i, j))} \quad (1) \quad S = \begin{bmatrix} I_x^2 & I_x I_y \\ I_y I_x & I_y^2 \end{bmatrix} \quad (2) \quad f'(i, j) = f(i, j)^{1/\kappa} \quad (3)$$

Fourth, content-adaptive mesh nodes were sampled from the feature map using the Floyd-Steinberg error diffusion algorithm [2] with serpentine scanning. Finally, cMESH generation was done with triangular elements in 2-D and tetrahedral elements in 3-D using the Delaunay tessellation method [3].

Results

Fig. 1 (a) shows a MR image of the head where a feature map was derived using Eq. (1) and Eq. (2). Fig. 1 (b) is a demonstrative example of cMESH in which content adaptiveness of meshes is clearly shown: coarse meshes were formed in the homogeneous regions and fine meshes in more complex regions. By extending the technique to the MR volume image, Fig. 2 shows 3D rendered MR volume in (a) and its content-adaptive meshes in (b). On the top slice, the characteristics of cMESH are obviously visible.

Conclusions

One of the critical limitations of FEA is overly created nodes and elements overwhelming computation. The content-adaptive mesh generator developed in this work offers an effective means of mesh generation that automatically produces optimal numbers of nodes and elements to represent a region of interest in MRI. The technique should be directly applicable to many fields where MR information-based finite element analysis is an effective tool.

References

- [1] T.-S. Kim et al., Proc. Int. Conf. IEEE Eng. Med. Biol., pp. 1880-1883, 2004
- [2] R. Floyd et al., SID Int. Symp. Digest of Tech. Papers, pp. 36-37, 1975
- [3] D. F. Watson, The Comp. Jour., vol. 24, no. 2, pp. 167-172, 1981

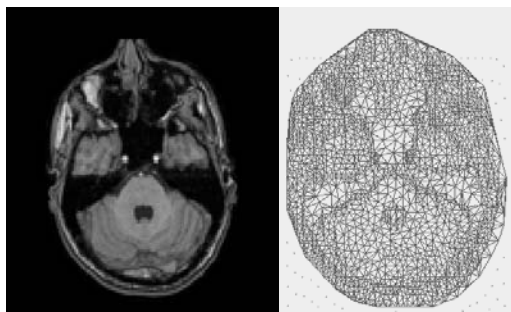


Fig. 1. (a) MR image and (b) Content-adaptive meshes from (a) with 2128 nodes and 4198 elements

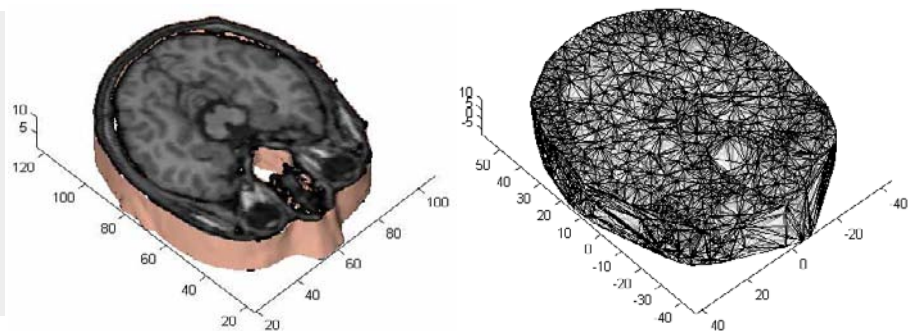


Fig. 2. (a) 3-D rendered head volume to be meshed and (b) 3-D content-adaptive meshes with 6054 nodes and 35195 tetrahedral elements.